

## Article

# Optimization of Synergetic Seismic and Energy Retrofitting Based on Timber Beams and Bio-Based Infill Panels: Application to an Existing Masonry Building in Switzerland

Simon Sanchez Zuluaga <sup>1</sup>, Stylianos Kallioras <sup>2</sup> and Anastasios Tsiavos <sup>1,\*</sup>

<sup>1</sup> Department of Civil, Environmental and Geomatic Engineering, ETH Zürich, 8093 Zürich, Switzerland; simonsa@student.ethz.ch

<sup>2</sup> Joint Research Center (JRC), 21027 Ispra, Italy; stylianos.kallioras@ec.europa.eu

\* Correspondence: tsiavos@ibk.baug.ethz.ch

**Abstract:** This paper presents an optimization process for the design of a novel synergetic seismic and energy retrofitting strategy that combines the favorable mechanical properties of timber and the attractive thermal insulation properties of bio-based materials. The novel method, defined as Strong Thermal and Seismic Backs (STSB), comprises the attachment of timber frames and bio-based thermal insulation panels on the vertical envelope and the facade walls of existing masonry buildings, thus improving both the seismic behavior and the energy performance of these buildings. This strategy is integrated and visualized in a novel synergetic framework for the holistic evaluation of the seismic behavior, the energy performance and the carbon footprint of existing buildings, defined as the Seismic and Energy Retrofitting Scoreboard (SERS). The benefit of the novel retrofitting strategy is quantified based on the numerical simulation of the seismic behavior of an unreinforced masonry building located in Switzerland, an assessment of the energy performance of the building and an evaluation of the carbon footprint of the proposed retrofit solution. Three retrofitting alternatives are investigated for the synergetic seismic and energy retrofitting of the building, comprising timber beams and two different bio-based materials for the thermal insulation of the vertical envelope of the building: cork and recycled natural grass. The optimal seismic and energy retrofitting strategy for the building among the alternatives assessed in this study is chosen based on a Multi-Criteria Decision Making (MCDM) procedure.

**Keywords:** synergetic seismic and energy retrofitting; masonry buildings; numerical simulation



**Citation:** Zuluaga, S.S.; Kallioras, S.; Tsiavos, A. Optimization of Synergetic Seismic and Energy Retrofitting Based on Timber Beams and Bio-Based Infill Panels: Application to an Existing Masonry Building in Switzerland. *Buildings* **2022**, *12*, 1126. <https://doi.org/10.3390/buildings12081126>

Academic Editor: Luca Pelà

Received: 17 June 2022

Accepted: 23 July 2022

Published: 29 July 2022

**Publisher's Note:** MDPI stays neutral with regard to jurisdictional claims in published maps and institutional affiliations.



**Copyright:** © 2022 by the authors. Licensee MDPI, Basel, Switzerland. This article is an open access article distributed under the terms and conditions of the Creative Commons Attribution (CC BY) license (<https://creativecommons.org/licenses/by/4.0/>).

## 1. Introduction

A significant part of the European residential building inventory, namely 30–40%, is located in regions of moderate to high seismic hazard [1]. However, a large percentage of these buildings are more than 50 years old and have not been designed for seismic actions. In Switzerland, more than 50% of the existing building inventory was constructed before the introduction of seismic code provisions in 1970 and roughly 90% was built before the introduction of the modern seismic code provisions in 2003.

Therefore, the majority of these buildings are seismically vulnerable and require an upgrade of their seismic performance. Calvi [2] stated that the performance-based retrofitting of existing buildings may lead to irrational cost-benefit ratios. Wenk [3] showed that the seismic retrofitting cost of buildings located in Switzerland is often not commensurate and can exceed 30% of the building value. A large amount of this portfolio of structures comprises unreinforced masonry buildings, whose seismic response is related to substantial uncertainties and high vulnerability [4–8]. The out-of-plane failure of unreinforced masonry buildings is a very common source of seismic damage for these buildings [9–11]. However, the high investment cost for the retrofitting of existing buildings cannot be easily justified based on the benefit obtained through the seismic risk reduction in these buildings after

the conduction of seismic retrofitting [12–14]. Moreover, the application of conventional strengthening techniques, such as steel, RC jacketing or RC walls placed around columns of existing buildings requires intensive labor, high cost, a substantial amount of materials related to high CO<sub>2</sub> emissions and does not allow the functionality of the building during the renovation [15]. Among other researchers, the use of Fiber Reinforced Polymers (FRP) has been proposed by Shing and Stavridis [16], Minafo et al. [17] and Aprile et al. [18] to reduce the number of resources needed for the retrofitting of existing masonry buildings. However, the environmental impact due to the use of polymer materials for the rehabilitation of existing buildings should be carefully considered.

The presence of a large number of old buildings in the existing European building inventory is not only related to high seismic vulnerability but has also a direct effect on the energetic efficiency of these buildings [19–22]. At a European level, the energy associated with the heating and cooling of the building inventory accounts for 40% of the total energy consumption and greenhouse gas emissions in Europe [23,24]. The World Meteorological Organization (WMO) reported that record atmospheric greenhouse gas concentrations and associated accumulated heat have propelled the planet into uncharted territory, with far-reaching repercussions for current and future generations [25]. This high energy demand is expected to increase during the next years due to the ageing and deterioration of the building inventory, unless a significant part of this inventory is renovated. However, the energy renovation during the last decades was limited to only 0.4–1.2% of the European building stock [26]. Moreover, Furtado et al. [27], Belleri and Marini [28], Formisano and Vaiano [29], Negro et al. [30] and Caprino et al. [31] demonstrated that the energy renovation of existing buildings does not typically consider structural deficiencies, which could leave the building seriously unsafe and inhibit the investment of retrofitting.

During the last five years, several studies have proposed combined retrofitting measures that simultaneously improve the seismic and energy performance of existing buildings. Triantafyllou et al. [32] investigated experimentally the use of Textile Reinforced Mortars (TRM) and thermal insulating materials, such as expanded polystyrene for the combined seismic and energy retrofitting of unreinforced masonry structures. Caruso et al. [33] proposed an integrated economic and environmental building classification as well as the combined seismic and energy retrofitting of RC buildings with RC walls and EPS panels or a thin layer of liquid ceramic insulation covering the vertical envelope of the building. Baek et al. [34] investigated experimentally a hybrid retrofit system consisting of prefabricated textile capillary-tube panels, mechanically connected through mortar or adhesives to existing building envelopes. Gkournelos et al. [35] have shown the shorter payback period of the integrated retrofitting techniques compared to conventional seismic or energy retrofitting methods, which are conducted independently.

A common theme across the aforementioned studies is the use of materials of high environmental impact and carbon footprint for the synergetic improvement of the seismic behavior and the energy performance of existing buildings. However, timber is a material of low environmental impact that can substantially decrease the carbon footprint of the retrofitting of existing structures [36–39]. Simões [40], Simões and Bento [41], Cardoso et al. [42] and Jiménez et al. [43] presented the beneficial characteristics of traditional timber-brick masonry construction consisting of burnt clay bricks filling in a framework of timber to create a patchwork of masonry, which is confined in small panels by the surrounding timber elements. Several researchers [44–46] have proposed the design of composite structures made of timber and concrete. Dizhur et al. [47] and Miglietta et al. [48] investigated experimentally the seismic retrofitting of masonry walls using timber frames to protect them from out-of-plane failure. However, the use of these timber frames only improves the seismic out-of-plane behavior of an existing masonry building, without affecting its thermal behavior. Moreover, the aforementioned timber frames were installed in the inner side of the building.

Along these lines, this paper aims to propose a novel seismic and energy retrofitting strategy that combines the favorable mechanical properties of timber and the attractive

thermal insulation properties of bio-based materials, thus improving both the seismic behavior and the energy performance of existing buildings. The benefit of this strategy for the synergetic retrofitting of existing buildings will be demonstrated through the numerical simulation of the seismic behavior and the energy performance of a masonry building located in Switzerland. Three retrofitting alternatives are investigated for the synergetic seismic and energy retrofitting of the building, comprising timber beams applied to the outer side of the facade walls and two different bio-based materials for the thermal insulation of the vertical envelope of the building: cork and recycled natural grass. The optimal seismic and energy retrofitting strategy for the building among the assessed alternatives will be chosen based on a Multi-Criteria Decision Making (MCDM) procedure. The improvement of the seismic and energy performance of the building compared to the unretrofitted building and the environmental advantages due to the use of low-carbon retrofitting methods will be illustrated using an assessment framework that can be used for the holistic evaluation of the seismic behavior, the energy performance and the carbon footprint of existing buildings, defined as the Seismic and Energy Retrofitting Scoreboard (SERS).

## 2. Modelling of the Unretrofitted Building

### 2.1. Case-Study Building

The case-study building is an unreinforced masonry, three-storey building located in Saint Gallen, Switzerland (Figure 1). The building was constructed in 1973, before the introduction of the seismic code provisions in Switzerland. The building consists of double-leaf unreinforced masonry walls at its perimeter with a thickness of 33 cm. The following assumptions were made about the mechanical properties of masonry: The modulus of elasticity was assumed as  $E = 3.5$  GPa, the shear modulus was assumed as  $G = 1.5$  GPa, the compressive strength was assumed as  $f_c = 1.3$  MPa and the cohesion of masonry was assumed as  $c = 0.33$  MPa [4]. The presented values were assumed based on examples of typical existing URM buildings located in Switzerland, due to the uncertainties related to the determination of the mechanical properties of the presented URM building. The effect of the variation of the selected mechanical properties on the presented results can be demonstrated by future investigations focusing on the different typologies of masonry buildings located in Switzerland and worldwide.

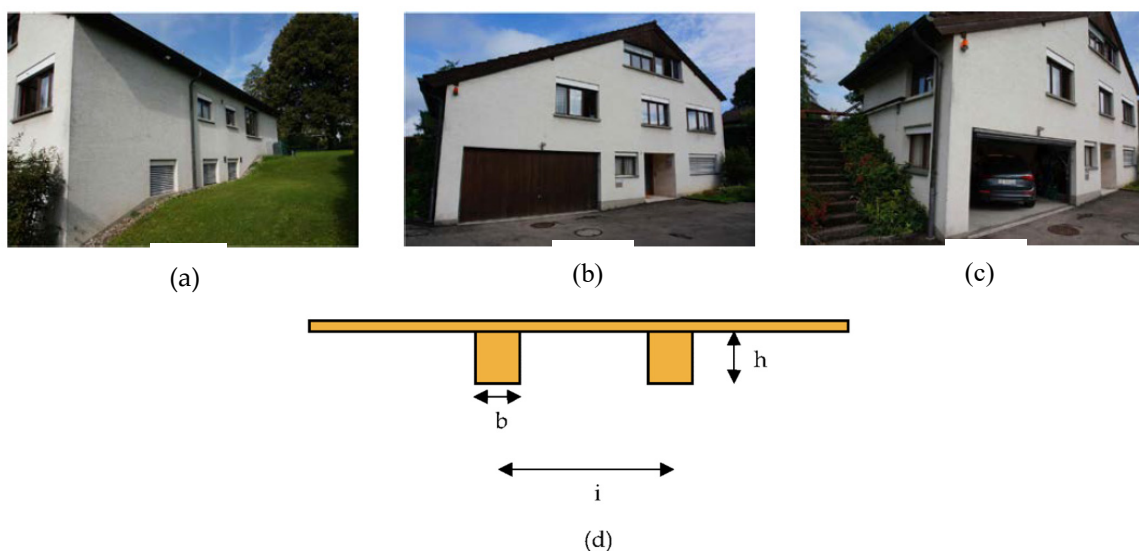


**Figure 1.** (a) North-east facade (b) south-east facade (c) south-west facade and (d) timber floor diaphragm of the building.

Due to lack of detailed information about the building and the low seismicity of Saint Gallen, the following assumptions were made for the building:

1. The building is located in Sion, which belongs to the seismic zone of the highest seismicity in Switzerland (Z3b) with  $PGA = 0.16 g$ .
2. The floors consist of timber beams with wooden planking, as shown in Figure 1d and Table 1.

**Table 1.** Floor system consisting of timber beams with wooden planking.

Timber Beams	
Beam width $b$	15 cm
Beam height $h$	20 cm
Beam spacing $i$	50 cm
Modulus of elasticity $E$	$6875 \text{ N/mm}^2$
Timber planking	
Thickness	4 cm
Shear modulus $G$	$10 \text{ N/mm}^2$

## 2.2. Numerical Simulation of the Out-of-Plane Seismic Behavior of the Unretrofitted Building

The determination of the out-of-plane deformability of the unretrofitted building was performed through dynamic analysis. The 8.3 m tall south-east URM facade of the building (Figure 2a) was selected as the structural system that is critical for the out-of-plane behaviour of the building based on its slenderness and number of openings. The numerical simulation of the out-of-plane seismic behavior of this facade of the building was performed using the research version of the software TreMuri, which is a computer program specifically developed for the structural and seismic analysis of masonry buildings. The TreMuri program, based on the equivalent frame modelling approach, includes several macroelement models for the simulation of masonry and non-masonry structural members [49–52]. Macroelements are 2D finite elements defined between two nodes belonging to the same wall. The numerical model of the facade of the unretrofitted building in TreMuri is presented in Figure 2b. The dashed lines represent the distance of the centroid of the macroelement from the nodes that define it. Macroelements noted with numbers only correspond to piers, while macroelements noted with the letter E and a number next to it correspond to spandrels. As shown in Figure 2b, the triangular part of the facade is simulated using a multi-orthogonal, macroelement-based discretization.

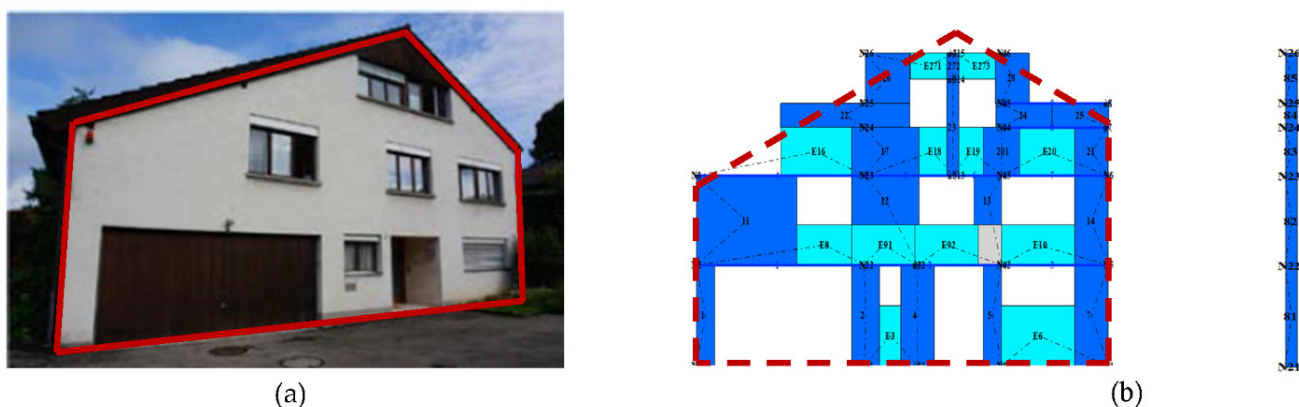


**Figure 2.** (a) South-east facade wall and (b) numerical model of the south-east facade wall in TreMuri.

The connection of the facade with the floors of the building was assumed to be very weak and is not simulated in the current numerical model. The determination of the out-of-plane deformation of the top of the facade for a wide range of seismic intensity levels was performed using Incremental Dynamic Analysis (IDA), as presented by Vam-

vatsikos and Cornell [53]. The model presented above was subjected to a ground motion ensemble comprising eight ground motion excitations, shown in Table 2. The selected earthquake ground motions are all recorded in Europe and cover a wide range of earthquake ground motion types (near- and far-field), magnitudes (5.0–6.5) and distances (10–60 km). The selected ground motion time histories were taken from the European Strong-Motion Database [54], the Italian Accelerometric Archive (ITACA) [55] and the PEER NGA Strong Motion Database [56].

**Table 2.** Ground motion ensemble used for the Incremental Dynamic Analysis.

No	Earthquake	Date	Station	Name	PGA-Recorded Motion (g)
1	Basso Tirreno, Italy	15.04.1978	Milazzo	MLZ000	0.07
2	Southern Italy	11.05.1984	Lazio Abruzzo	D-VLB000	0.15
3	Kalamata, Greece	15.09.1986	Messini-Town Hall	MES-NS	0.16
4	Kozani, Greece	13.05.1995	Kozani	KOZ-L	0.14
5	Imotski, Croatia	23.05.1974	Imotsko-Sum. Gos.	IMO	0.15
6	Friuli, Italy	06.05.1976	Buia	FRIULI -BUI000	0.14
7	Umbria-Marche, Italy	03.04.1998	Gubbio-Piana	UBMARCHE. NCB000	0.15
8	Sicilia-Orientale, Italy	13.12.1990	Sortino	SICORIEN.P_SRT-UP	0.18

The first three vibration periods of the facade wall out of its plane are shown in Table 3 below:

**Table 3.** First three vibration periods of the facade wall out of its plane.

	T1 (s)	T2 (s)	T3 (s)
Unretrofitted building	0.443	0.418	0.267
Retrofitted building	0.276	0.203	0.129

For each set of parameters, the modal properties were calculated first and then the Rayleigh damping model parameters were computed such that the damping ratios at the first and second mode corresponded to a damping coefficient of 5% [4]. The mean IDA curve of the facade out of plane subjected to Incremental Dynamic Analysis is presented in Figure 3.

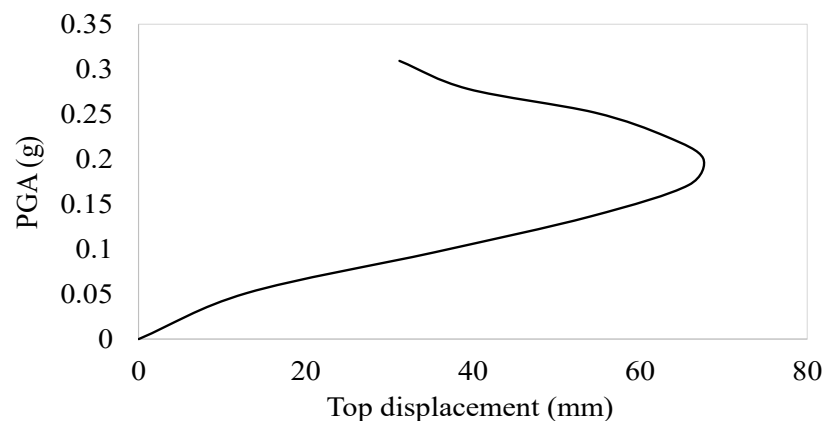


**Figure 3.** Mean out-of-plane IDA curve of the unretrofitted facade of the building.

As shown in Figure 3, the maximum out-of-plane displacement of the top of the facade wall is 68 mm for a seismic intensity of 0.2 g. The energy performance of the building was determined using the open-source software Ubakus [57], which focuses on the energy assessment of existing buildings. The total heating demand of the building was calculated



as  $Q_{ex} = 38537$  kWh/year. The operational carbon emissions per kWh heating oil are estimated according to Stolz and Frischknecht [58]:

$$\text{Carbon emissions per kWh heating oil} = 0.084 \frac{\text{kg CO}_2\text{eq}}{\text{MJ}} \cdot 3.6 \frac{\text{MJ}}{\text{kWh}} = 0.3 \frac{\text{kg CO}_2\text{eq}}{\text{kWh}} \quad (1)$$

The annual equivalent carbon emissions  $C$  due to the operation of the building can, therefore, be estimated as:

$$C = 38537 \text{ kWh} \cdot 0.3 \frac{\text{kg CO}_2\text{eq}}{\text{kWh}} = 11654 \frac{\text{kg CO}_2\text{eq}}{\text{year}}$$

The maximum permissible energy requirement for new buildings located in Switzerland is calculated according to the Swiss Norm SIA 380/1 [59] as a function of the ratio of the thermal building envelope area  $A_{th}$  to the energy reference area  $A_E$ . The energy reference area of the building  $A_E$  is  $238.2 \text{ m}^2$ , while the thermal building envelope area  $A_{th}$  is  $531.2 \text{ m}^2$ , thus leading to  $A_{th}/A_E = 2.23$  and a maximum permissible energy requirement for a new building  $Q_{new} = 11284$  kWh/year. The energy compliance factor of an existing building  $\alpha_E$  is defined as the ratio of the heating demand required for a new building  $Q_{new}$  compared to the heating demand of the existing building  $Q_{ex}$ :

$$\alpha_E = \frac{Q_{new}}{Q_{ex}} \quad (2)$$

This dimensionless ratio, which has been used to quantify the energy performance of the existing URM building in this study, was calculated as  $\alpha_E = 11,284 \text{ kWh/year} / 38,537 \text{ kWh/year} = 0.29 = 29\%$ . Therefore, the existing building does not meet the energy requirements for new buildings located in Switzerland and can be considered as energy deficient.

### 3. Modelling of the Retrofitted Building

#### 3.1. Synergetic Seismic and Energy Retrofitting Strategy

The carbon content of bio-based materials corresponds to approximately 50% of their total mass, thus offering an opportunity for  $\text{CO}_2$  storage over an extended period of time when used as a building material [60,61].

Grass is a bio-based material of negative carbon footprint, which is naturally abundant all over the world and has excellent thermal insulation properties: The European Technical Approval for Grass Insulation declares a thermal conductivity of  $0.040 \text{ W/mK}$  for grass density between  $30$  and  $80 \text{ kg/m}^3$  [62]. Grass is not affected by temperature or moisture variations and is recyclable [62]. The attachment of pressed grass panels obtained from waste natural grass [63] on the vertical envelope of existing buildings facilitates their efficient thermal insulation, while minimizing the environmental impact of the energy upgrade.

Cork is a highly durable material with a lifespan longer than 50 years. It has thermal conductivity of  $0.040 \text{ W/mK}$  for density  $110 \text{ kg/m}^3$  [64]. Furthermore, cork is waterproof, low-cost, resistant to fungi, recyclable, biodegradable and is associated with low carbon ( $\text{CO}_2$ ) emissions: when the cork is harvested the trees are not cut down, instead their bark is carefully stripped away by hand. Last but not least, cork composites can be produced from the leftovers of bottle stoppers production. These boards are ground to specific granule size and mixed with a specific resin [65].

The synergetic seismic and energy retrofitting strategy proposed in this study combines the favorable role of the use of timber frames for the seismic out-of-plane protection of masonry buildings with the thermal and environmental benefits due to the use of bio-based insulation for the upgrade of the energy performance of these buildings. This combined seismic and energy retrofitting strategy, defined as Strong Thermal and Seismic Backs (STSB) entails the attachment timber frames infilled with bio-based thermal insulation panels on

the outer surface of the facade of an existing masonry building. The layer configuration for the installation of this combined seismic and energy retrofitting strategy and its application on the south-east facade of the masonry building presented in Figure 1b are shown in Figures 4 and 5, respectively. A vapor retarder is used between the inner surface of the bio-based thermal insulation and the existing masonry walls to impede moisture flow and protect from damage caused by condensation. As shown in Figure 4, two different bio-based thermal insulation layers are used for the upgrade of the energy behavior of the building: cork boards and pressed grass panels obtained from recycled natural grass [63].

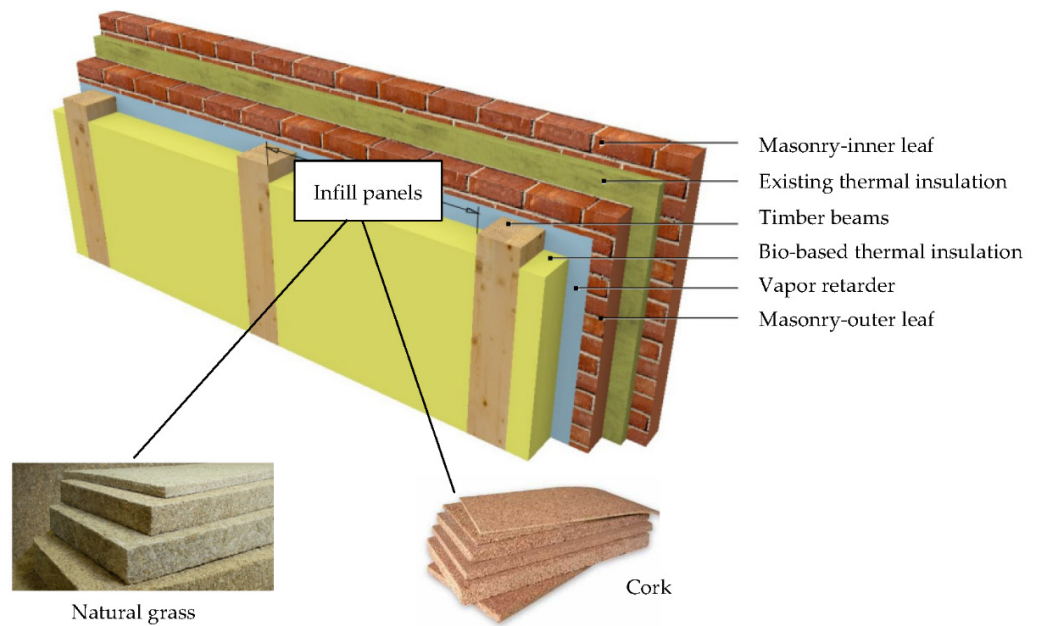


**Figure 4.** Layer configuration for the installation of Strong Thermal and Seismic Backs using two alternatives for bio-based thermal insulation infill panels: natural grass and cork.

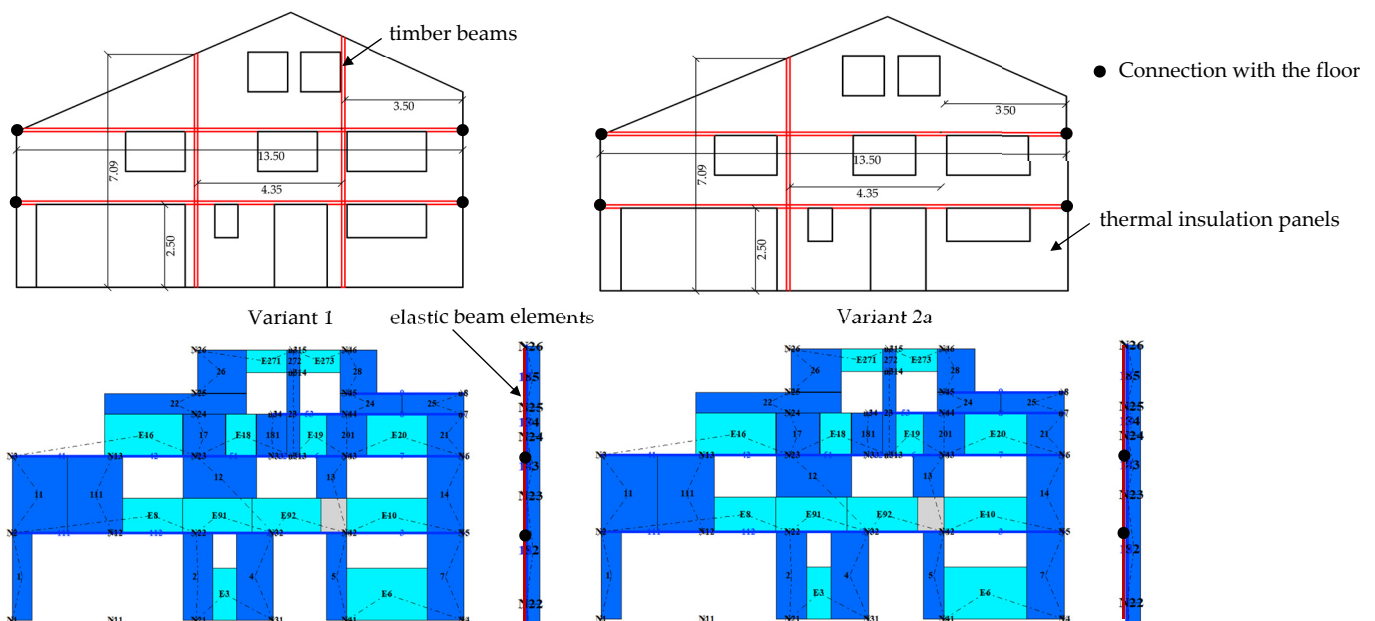


**Figure 5.** Presentation of the two different variants (Variant 1, Variant 2a) for the seismic retrofitting of the south-east URM facade and the corresponding numerical models that simulate the seismic out-of-plane response of the retrofitted building.

### 3.2. Retrofitting Alternatives

Three retrofitting alternatives have been designed for the synergetic seismic and energy retrofitting of the building, comprising 10 cm × 10 cm timber beams (Figure 6c) and two different bio-based materials for the thermal insulation of the vertical envelope of the building: cork and natural grass. The two different timber beam configurations that are designed to prevent the seismic out-of-plane failure of the critical south-east URM facade of the building (Figure 1b) and the corresponding numerical models using the research version of the software TreMuri [49–52] are shown in Figure 5. The timber beams have been modelled using elastic beam (flexural) elements (marked in red in Figure 5).

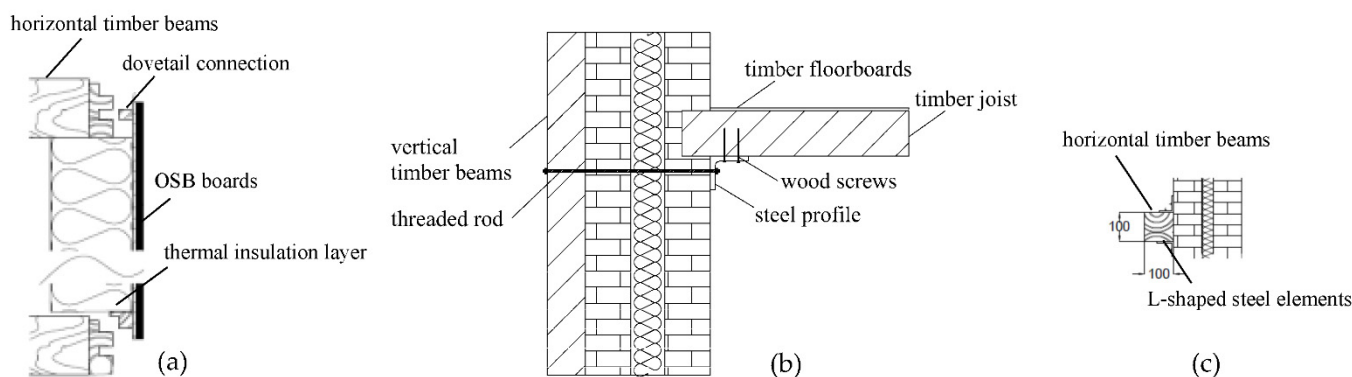


**Figure 6.** Design plans for the implementation of the presented seismic and energy retrofitting strategy: (a) Panel configuration (b) Connection with the floors (c) Connection with the facade wall (dimensions in mm).

The first two retrofit alternatives shown above (Variant 1, Variant 2a) entail the use of 17.5 cm-thick recycled waste natural grass panels [63] (Figure 4) as thermal insulation for the energy upgrade of the building. A third retrofitting alternative (Variant 2b), which comprises the timber beam configuration of Variant 2a but a different thermal insulation material, is explored: this alternative consists of 17.5 cm-thick cork panels (Figure 4) as thermal insulation for the energy upgrade of the building. The design of the proposed preassembled panels and their connection with the timber beams is shown in Figure 6.

As presented in Figure 6, the seismic and energy retrofitting strategy comprises horizontal and vertical timber beams, which are fixed to the masonry facade and the floors of the building through L-shaped steel elements [66] and threaded steel tie rods (Figure 6b,c). The boundary conditions indicating the points of the connection of the proposed retrofit with the floors of the building are shown in Figure 5. The 17.5 cm-thick bio-based thermal insulation layers are attached to OSB (Oriented Strand Board) panels, which are connected with the 10-cm thick horizontal timber beams through dovetail joints (Figure 6a). This modular configuration comprising the preassembled panels with the OSBs and the thermal insulation layers, which are connected in situ with the horizontal timber beams through dovetail joints, facilitates the efficient installation of the proposed retrofitting design on the outer facade of existing masonry buildings.

### 3.3. Numerical Simulation of the Out-of-Plane Seismic Behavior of the Retrofitted Building

The determination of the out-of-plane deformation of the top of the retrofitted facade for a wide range of seismic intensity levels was performed using Incremental Dynamic Analysis (IDA), as presented by Vamvatsikos and Cornell [53]. The numerical model presented above was subjected to the ground motion ensemble comprising eight ground motion excitations, which was presented in Table 2. The mean IDA curve of the retrofitted facade out of plane and its comparison with the IDA curve of the unretrofitted facade (Variants 1 and 2a) are presented in Figure 7.



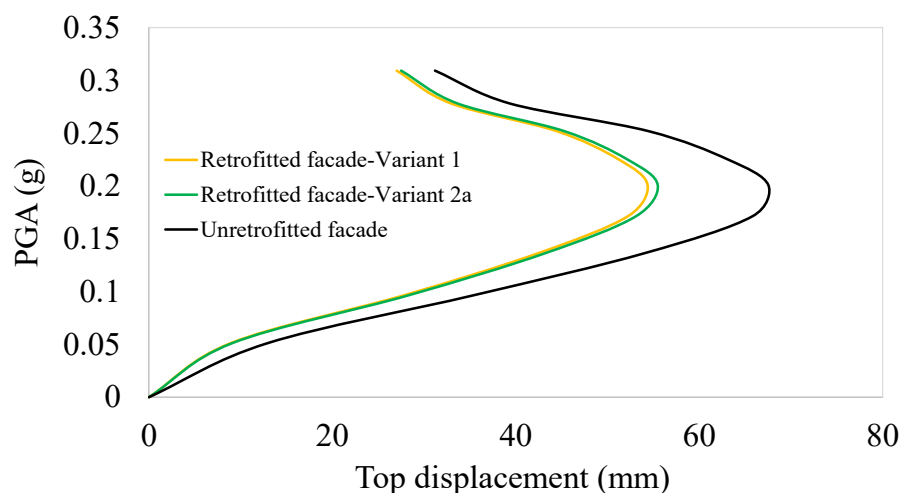


**Figure 7.** Mean out-of-plane IDA curve of the retrofitted facade of the building and comparison with the unretrofitted facade.

The displacement time history response of the top of the unretrofitted and retrofitted facade (retrofit variants 1 and 2a), subjected to the acceleration ground motion recorded at the at the 1974 Imotski earthquake (No 5 in Table 2) with scaled PGA = 0.2 g is shown in Figure 8 below.

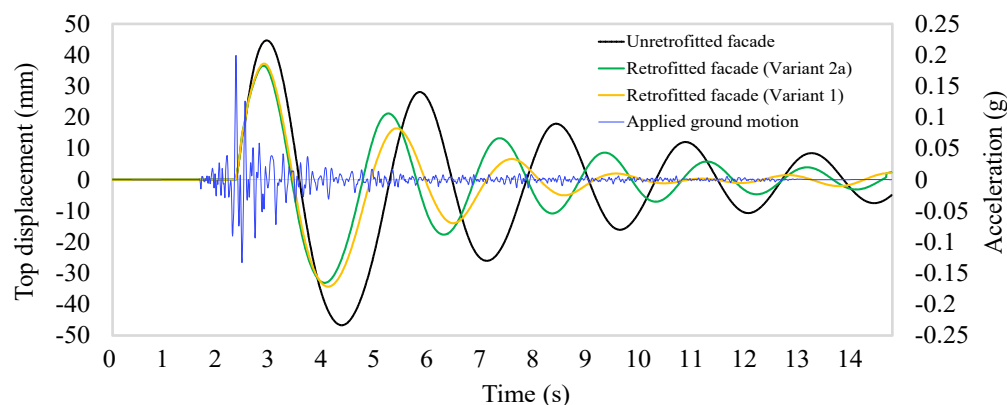


**Figure 8.** Displacement time history response of the unretrofitted and retrofitted facade (Variants 1 and 2a) subjected to the ground motion recorded at the 1974 Imotski earthquake (No 5 in Table 2) with PGA = 0.2 g.

As shown in Figures 7 and 8, both variants of the retrofitted facade manifested substantially smaller peak out-of-plane displacement than the unretrofitted facade, thus demonstrating the efficiency of the presented retrofitting strategy in reducing the out-of-plane displacement of the facade wall. The reduction in this out-of-plane displacement of the top of the facade wall is higher for Variant 1 (22% reduction compared to 20% obtained by Variant 2a, as shown in Figure 7) due to the higher amount of vertical timber beams that are attached to the facade in this structural configuration compared to Variant 2a.

### 3.4. Heating Demand of the Building before and after the Retrofitting

The heating demand of the building before and after the retrofitting was calculated using the energy assessment software Ubaqus [57] and is presented in Figure 9. The annual equivalent carbon emissions  $C$  due to the operation of the unretrofitted building are 11,654 kg CO<sub>2</sub>-eq/a. The application of the synergetic retrofitting variants 1 and 2a, which are based on the same thermal insulation material (recycled natural grass) on the vertical envelope of the building led to the same value of the operational carbon emissions

of the building, corresponding to 8316 kg CO<sub>2</sub>-eq/a and 28.6% reduction compared to the unretrofitted building. The use of cork as a thermal insulation layer applied for the retrofitting variant 2b led to the same value of the operational carbon emissions of the building due to the same thermal conductivity (U-value) of cork (0.040 W/mK) with the corresponding value of the recycled natural grass.

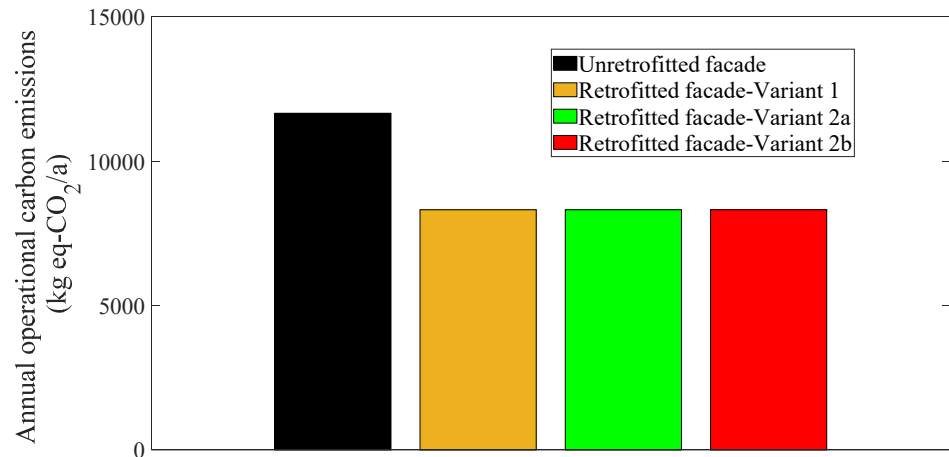


**Figure 9.** Comparison between the operational carbon emissions of the unretrofitted and the retrofitted building for the three retrofitting alternatives.

### 3.5. Embodied Carbon Emissions of the Synergetic Retrofitting Strategies

The embodied carbon emissions of the materials that are chosen for the implementation of the synergetic retrofitting strategies shown in this study are presented in Figure 10. As shown in the figure, the use of the bio-based materials presented in this study leads to negative carbon emission values for all the retrofitting variants, thus demonstrating the sustainability of the synergetic retrofitting solutions comprising timber and bio-based thermal insulation panels. However, the retrofitting variant 2b, comprising the use of timber beams and cork insulation panels, manifests substantially lower (negative) embodied carbon emission values compared to the other two variants, which correspond to the maximum storage of CO<sub>2</sub> by the materials and the lowest environmental impact among the three retrofitting solutions. This beneficial behavior of variant 2b is attributed to the ability of cork to store large amounts of CO<sub>2</sub> during its use, thus contributing to the reduction in carbon emissions in the atmosphere and the mitigation of the consequences of climate change.

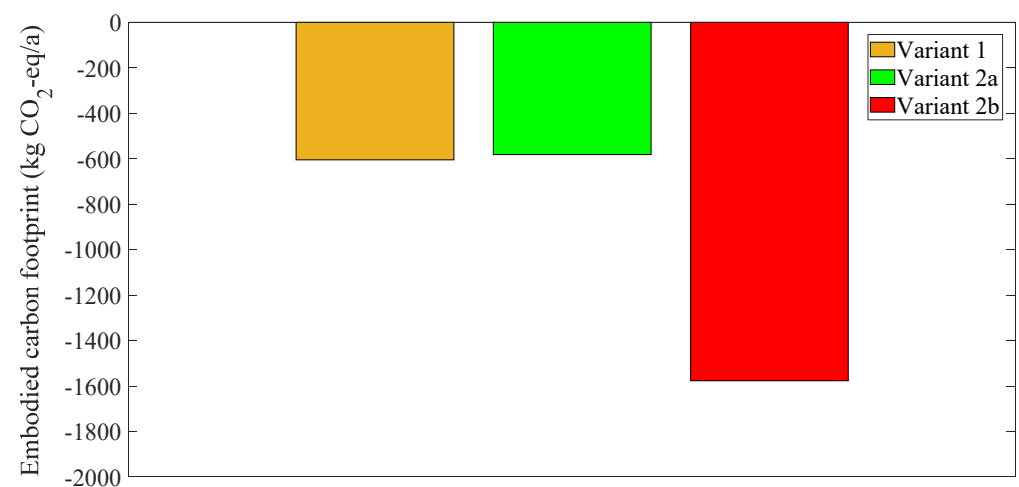


**Figure 10.** Embodied carbon emissions of the three synergetic retrofitting alternatives.

#### 4. Seismic and Energy Retrofitting Scoreboard (SERS)

A novel assessment framework is proposed in this study for the combined evaluation of the seismic behavior, the energy performance and the environmental impact of an existing building before and after the retrofitting, as well as the multi-performance comparison of different synergetic retrofitting strategies. This framework is defined as the Seismic and Energy Retrofitting Scoreboard (SERS). The framework proposes the use of a rating system that utilizes performance metrics and awards points (from 1 point to 7 points) for the performance of the building in four different aspects: the seismic behavior of the building, the heating demand of the building (related to its operational carbon emissions), the embodied carbon emissions and the cost of retrofitting. Four different performance metrics have been used in this study:

- a. The normalized reduction in the seismic out-of-plane displacement of the building  $\alpha_S$  due to retrofitting, defined as follows:

$$\alpha_S = \frac{|\text{Maximum Displacement after retrofitting}| - |\text{Maximum Displacement before retrofitting}|}{|\text{Maximum Displacement before retrofitting}|} \quad (3)$$

- b. The energy compliance of the building  $\alpha_E$  (Equation (2)).
- c. The embodied carbon emissions of retrofitting, defined in kg CO<sub>2</sub>-eq/a.
- d. The construction and installation cost of the retrofitting strategy.

The following Table 4 shows the values of these parameters for the three retrofitting strategies presented in this study. The rating system of the Seismic and Energy Retrofitting Scoreboard (SERS) is presented in Table 5.

**Table 4.** Performance indicators for the three retrofit alternatives presented in this study.

Variable	Retrofit Variant 1	Retrofit Variant 2a	Retrofit Variant 2b
Normalized out-of-plane displacement reduction $\alpha_S$	22%	20%	20%
Energy compliance $\alpha_E$	140%	140%	140%
Embodied carbon emissions (kg CO <sub>2</sub> -eq/a)	−605	−582	−1577
Installation cost (EUR)	33,300	32,455	35,640

**Table 5.** Seismic and Energy Retrofitting Scoreboard (SERS): rating system.

Class	Points in Scoreboard	Normalized Out-of-Plane Displacement Reduction $\alpha_S$	Energy Compliance $\alpha_E$	Embodied Carbon Emissions kg CO <sub>2</sub> -eq/a	Cost (EUR)
A	7	>30%	>200%	<−1500	10,000–30,000
B	6	25–30%	100–200%	−1500 to −1000	30,000–50,000
C	5	20–25%	80–100%	−1000 to −500	50,000–100,000
D	4	15–20%	60–80%	−500 to 0	100,000–200,000
E	3	10–15%	40–60%	0 to 500	200,000–300,000
F	2	5–10%	20–40%	500 to 1000	300,000–500,000
G	1	0	0–20%	>1000	>500,000

According to the points obtained in each of the four aforementioned aspects, the performance of the building is divided into seven classes (A class to G class), presented with different colors in Table 5.

The performance of the building before and after the retrofitting considering its seismic behavior, its energy compliance and its operational carbon footprint using the SERS assessment framework is presented in Figure 11. The same values of these performance metrics apply for all retrofitting strategies selected in this study, as they all lead to the same seismic performance and heating demand (or operational carbon footprint) after the retrofitting (Figure 9, Tables 4 and 5). However, a more detailed comparison between

the different retrofitting strategies considering their embodied carbon emissions and their cost, presented in Figure 12, elucidates the optimal synergetic retrofitting solution for the building among all the alternatives assessed in this study.

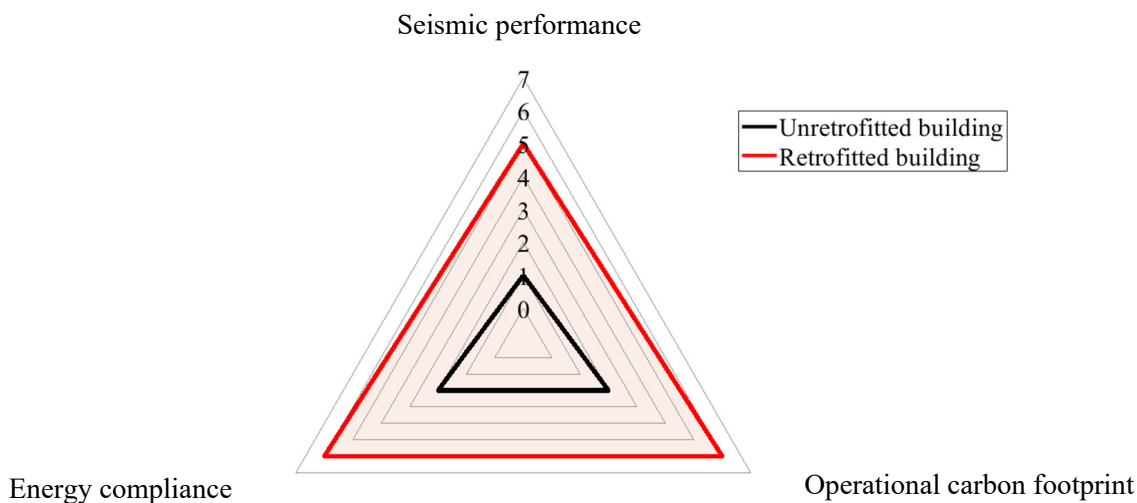


**Figure 11.** Seismic and Energy Retrofitting Scoreboard: assessment of the unretrofitted and the retrofitted building.

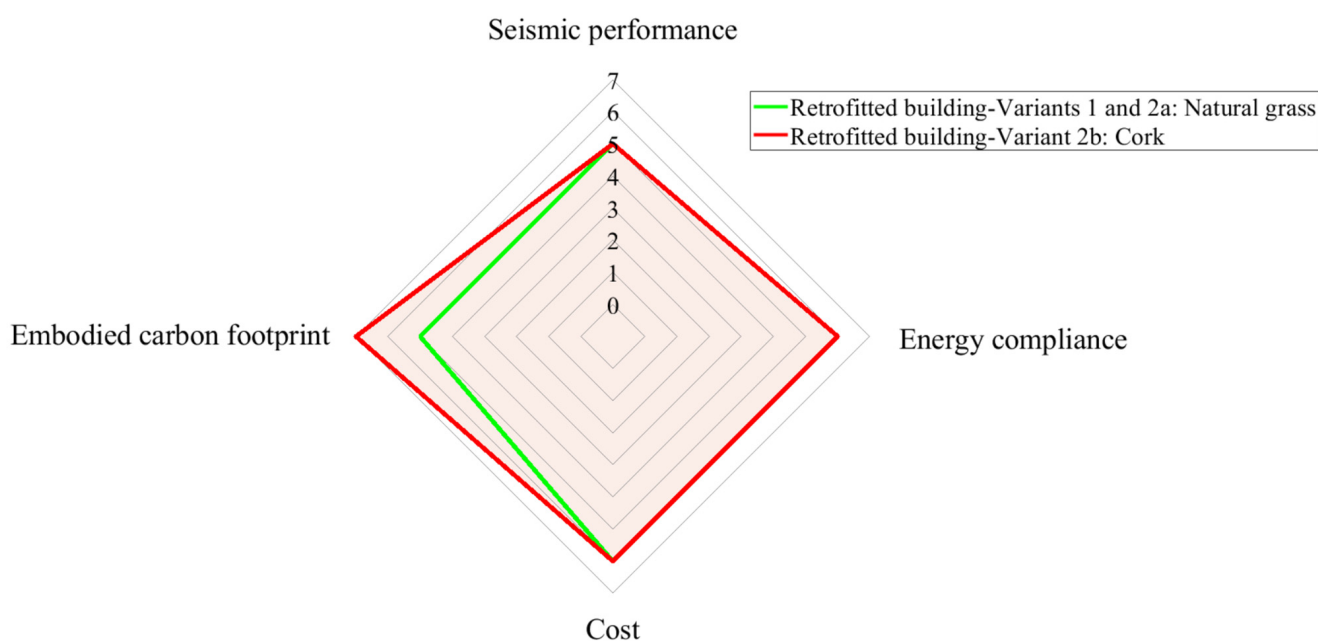


**Figure 12.** Seismic and Energy Retrofitting Scoreboard: assessment of the different retrofitting strategies.

As shown in Figure 12, the retrofitting variant 2b, comprising timber beams and cork thermal insulation panels, leads to the maximum area in the inner side of the trapezoidal curve that represents the multi-performance assessment of the retrofitting strategies. This representation illustrates the advantages of this retrofitting strategy compared to the other two strategies explored in this study: the installation of cork panels as thermal insulation at the vertical envelope of the building leads to the lowest embodied carbon emissions due to the ability of cork to store CO<sub>2</sub>, manifested by the negative carbon footprint of the material (Table 4). The retrofitting variants 1 and 2a lead to the same multi-performance assessment rating, thus, they are represented with the same green line in Figure 12.

## 5. Determination of the Optimal Retrofitting Strategy Based on Multi-Criteria-Decision Making (MCDM) Process

The determination of the optimal retrofitting strategy among the assessed options was also performed analytically through a Multi-Criteria Decision Making process (MCDM) using a process similar to the one followed by Carofilis et al. [67] and Clemett et al. [23], whose application was presented in detail by Caterino et al. [68] and Santarsiero et al. [69]. The four decision variables that were chosen to assess the performance of the three retrofit alternatives are: the seismic performance of the building (P1) expressed by the normalized out-of-plane displacement reduction  $\alpha_s$ , the embodied carbon footprint of retrofitting (P2) defined by the embodied carbon emissions of retrofitting (kg CO<sub>2</sub>-eq/a), the energy compliance (P3) defined by Equation 2 and the installation and construction cost of retrofitting (P4) in EUR. The relative importance of each of these parameters is shown in Table 6. The weight factors shown in Table 6 place more emphasis on the seismic behavior and the energy performance of the building and are chosen in a different manner than the weight factors selected by Gentile and Galasso [70], which place higher importance to the installation cost of the retrofitting measures.

**Table 6.** Decision variables for the three retrofit alternatives presented in this study.

Variable	Relative Importance
P1: Seismic performance	0.48
P2: Embodied carbon footprint	0.16
P3: Energy compliance	0.24
P4: Cost	0.12

The values that indicate the relative closeness of each retrofit variant to the fictitious ‘ideal’ retrofit solution are shown in Table 7 in preferential order (I corresponds to the optimal solution among the assessed options, III corresponds to the least optimal solution among the assessed options). The relative closeness values lie in the range (0, 1), with a value of 1 indicating that an alternative is the ‘ideal’ solution. The difference between the relative closeness values can be used to quantify the preference of one alternative over the other alternative [23,71]. As shown in Table 7, the retrofit variant 2b is the optimal retrofit solution among the assessed variants, due to the ability of cork to store the highest amount of CO<sub>2</sub> manifested by the negative carbon footprint of the material (Table 4). The retrofit variant 2a yields slightly better results than variant 1 due to the attractively minimal use of timber in the facade for the improvement of the seismic out-of-plane behavior of the building, which leads to similar reduction in out-of-plane displacement with variant 1. These results are in agreement with the results obtained through the maximization of the area obtained through the Seismic and Energy Retrofitting Scoreboard (SERS) shown in Figure 12, which also demonstrates the attractive characteristics of retrofit variant 2b as the optimal retrofit solution among the assessed variants.

**Table 7.** Ranking of the retrofit variants according to the MCDM process.

Retrofit Variant		
I	II	III
Retrofit variant 2b	Retrofit variant 2a	Retrofit variant 1
0.955	0.849	0.839

## 6. Conclusions

This paper presents an optimization process for the design of a novel seismic and energy retrofitting strategy that combines the favorable mechanical properties of timber and the attractive thermal insulation properties of bio-based materials. The novel method,



defined as Strong Thermal and Seismic Backs (STSB), comprises the attachment of timber frames and bio-based thermal insulation panels on the vertical envelope and the facade walls of existing masonry buildings, thus improving both the seismic behavior and the energy performance of these buildings. This strategy is integrated in a novel synergetic framework for the holistic evaluation of the seismic behavior, the energy performance and the carbon footprint of existing buildings, defined as the Seismic and Energy Retrofitting Scoreboard (SERS).

The efficiency of the method in the simultaneous improvement of the seismic behavior and the energy performance of existing buildings was demonstrated through the numerical simulation of the seismic behavior and the energy performance of an unreinforced masonry building located in Switzerland. The simulation of the out-of-plane seismic behavior of the building before and after the retrofitting was performed using the research version of the software TreMuri. The assessment of the heating demand and the operational carbon emissions of the building before and after the retrofitting was performed using the software Ubaqus to determine the energy performance and the environmental impact during the operation of the building before and after the retrofitting. The embodied carbon emissions of retrofitting were quantified to assess the environmental impact of the retrofitting method attributed to the selected materials.

Three retrofitting alternatives were investigated for the synergetic seismic and energy retrofitting of the building, comprising timber beams and two different bio-based materials for the thermal insulation of the vertical envelope of the building: cork and recycled natural grass. The first two alternatives (1, 2a) entail the use of 17.5 cm-thick recycled waste natural grass panels as thermal insulation for the energy upgrade of the building, while consisting of different geometrical configurations for the attachment of 10 cm × 10 cm timber beams to the facade wall to protect it from out-of-plane failure during an earthquake excitation. A third retrofitting alternative 2b, which comprises the timber beam configuration of Variant 2a but a different thermal insulation material, is explored: this alternative consists of 17.5 cm-thick cork panels (Figure 4) as thermal insulation for the energy upgrade of the building. The reduction in the out-of-plane displacement of the top of the facade wall is higher for Variant 1 (22% reduction compared to 20% obtained by Variant 2a, as shown in Figure 7) due to the higher amount of vertical timber beams that are attached to the facade in this structural configuration, compared to Variant 2a.

The presented synergetic seismic and energy retrofitting strategy can only improve the energy performance of the building if applied at the building envelope. However, as shown by Miglietta et al. [47], the attachment of timber beams to existing masonry walls can increase both the in-plane and the out-of-plane strength of these walls. Within this frame, even if applied at the building envelope, the method could improve substantially both the local and the global (in-plane and out-of-plane) seismic behavior of existing masonry buildings, comprising a URM lateral load resisting system that is concentrated at the building envelope. In case the lateral load resisting system of the building is mainly located internally in the building, the presented method comprising the attachment of timber beams can still be applied without the addition of thermal insulation, thus improving globally the seismic behavior of the building. However, if the method is applied internally at the building and not at its envelope, it cannot substantially influence the energy behavior of the building, as the majority of heating losses arises mainly through the envelope of existing buildings.

The use of 17.5 cm-thick thermal insulation panels constructed from two different bio-based materials, cork and recycled natural grass, led to almost the same value of 30% decrease in the heating demand and the annual operational carbon emissions of the building, compared to the unretrofitted case. The use of both materials leads to negative embodied carbon footprint values, thus decreasing substantially the environmental impact of retrofitting, compared to conventional energy retrofitting methods. However, the use of cork leads to 1.6 times lower (more negative) carbon footprint values than natural grass,

thus showing the ability of the material to store a higher amount of CO<sub>2</sub> within the same time frame.

The improvement of the seismic and energy performance of the building compared to the unretrofitted building and the environmental advantages due to the use of low-carbon retrofitting methods are integrated and visualized in a novel assessment framework that can be used for the holistic evaluation of the seismic behavior, the energy performance and the carbon footprint of existing buildings, defined as the Seismic and Energy Retrofitting Scoreboard (SERS). This framework proposes the use of a rating system that utilizes performance metrics and awards points (0–7) for the performance of the building in four different aspects: the seismic behavior of the building, the heating demand of the building (related to its operational carbon emissions), the embodied carbon emissions and the cost of retrofitting. A dimensionless factor, defined as energy compliance, is used to compare the energy performance of the building with the energy performance of a new building with the same dimensions, designed in the same location. The results of the rating are visualized using a spider-web-shaped diagram with four axes. Within this frame, the optimal retrofitting solution among the assessed variants can be illustrated through the maximization of the inner area of the trapezoidal curve that corresponds to the rating of the retrofitting of the building. The retrofit variant comprising the installation of timber beams and cork thermal insulation panels at the vertical envelope of the building (Variant 2b) leads to the maximum rating of 7 regarding the aspect ‘Embodied carbon footprint’ and the maximum inner area in the Figure, while the two other retrofit variants (1, 2a) lead to a lower rating in this aspect, equal to 5. The rating of all retrofit variants presented in this study considering the other performance aspects (seismic performance, energy compliance, cost) using the SERS framework is the same.

The visualization of the optimal results through the presented Seismic and Energy Retrofitting Scoreboard (SERS) can be used by the local authorities to assess multiple aspects of the performance of existing buildings, while considering different dimensionless parameters, such as the energy compliance of existing buildings proposed in this study. The aforementioned multi-performance representation can be further extended in the future to consider the seismic code compliance of existing buildings and their corresponding seismic risk, following the fragility curves and the seismic collapse risk estimation for varying values of seismic code compliance determined by Tsiavos et al. [12] for existing Reinforced Concrete (RC) buildings.

The optimal seismic and energy retrofitting strategy for the building among the assessed options is also quantified analytically based on a Multi-Criteria Decision Making (MCDM) procedure. The retrofit variant comprising the installation of timber beams and cork thermal insulation panels in the vertical envelope of the building is determined as the optimal retrofit solution, due to the ability of cork to store higher amounts of CO<sub>2</sub> manifested by the negative carbon footprint of the material.

This synergetic retrofitting strategy is not only applicable to Switzerland, but to many countries worldwide (e.g., Italy, Greece, Portugal, Turkey, New Zealand), whose building inventory comprises mainly unreinforced masonry buildings that are seismically vulnerable and energy deficient. The presented Multi-Criteria Decision Making process (MCDM) has been used in this study to indicate the optimal solution among three retrofit alternatives for a specific case-study, an unreinforced masonry building located in Switzerland. The consideration of more decision variables, more building types and more locations corresponding to different seismic hazard levels by future investigations would facilitate the integration of the presented optimization methodology in a wider context and the applicability of the presented retrofit solution to a broader spectrum of countries worldwide. Within this frame, this study could be extended to include the consideration of seismic resilience of existing buildings, as proposed by Carofilis et al. [71]. Last but not least, the effect of the connection of the facade with the floors of the building [72] and the flexibility of the diaphragm of the building on its seismic out-of-plane response could be investigated by future studies.

The proposal of the aforementioned synergetic retrofitting methods aims to lead to a paradigm shift in the maintenance and upgrade of the existing building inventory. The need for reduction in global carbon emissions, exacerbated by the global heating energy crisis, requires the simultaneous consideration of multiple aspects in the ways we design and retrofit our buildings. Within this frame, the prioritization of the retrofitting of our existing infrastructure should be based on performance objectives defined by our communities, which consider simultaneously the seismic vulnerability, the energy performance and the carbon emissions of our existing infrastructure within the context of the current climate change and energy crisis.

Along these lines, the retrofitting strategy and the holistic assessment framework proposed in this study aim to respond to this challenge through the combined seismic and energy retrofitting of existing buildings using sustainable materials, thus increasing the protection of our existing building inventory from seismic damage and mitigating the consequences of climate change and energy crisis.

**Author Contributions:** Conceptualization, A.T.; methodology, A.T.; software, S.K.; validation, A.T.; formal analysis, S.S.Z.; investigation, S.S.Z.; resources, A.T.; data curation, A.T.; writing—original draft preparation, A.T.; writing—review and editing, A.T.; visualization, A.T.; supervision, A.T.; project administration, A.T.; funding acquisition, A.T. All authors have read and agreed to the published version of the manuscript.

**Funding:** This research received no external funding.

**Institutional Review Board Statement:** Not applicable.

**Informed Consent Statement:** Not applicable.

**Acknowledgments:** The research work presented in this study was performed during Spring Semester 2022. We would like to thank Professor Andrea Penna (University of Pavia), Professor Sergio Lagomarsino (University of Genoa), Dr. Alessandro Galasco (University of Pavia) and Professor Serena Cattari (University of Genoa) for providing us licenses for the research version of TreMuri. Professor Arno Schlueter (Chair of Architecture and Building Systems at ETH Zurich), Dr. Illias Hischier (ETH Zurich) and Mr. Diego Sigrist are kindly acknowledged for their advice related to the simulation of the energy performance of the building. We also thank Dr. Francesco Vanin (EPFL Lausanne), Mr. Safak Arslantürkoglu (ETH Zurich), Mr. Remo Huesser, Mr. Igor Tomić (EPFL Lausanne), Dr. Yves Reuland (ETH Zurich), and Ms. Nathalie Reckinger (ETH Zurich) for their contribution to this study. Ms. Alina Galimshina is kindly acknowledged for her advice related to the calculation of the carbon footprint of the presented retrofitting strategy. Last but not least, we would like to thank Mr. Dominik Bissig and Dr. Stephan Schilling for their advice related to timber structures.

**Conflicts of Interest:** The authors declare no conflict of interest.

## References

1. Crowley, H.; Despotaki, V.; Rodrigues, D.; Silva, V.; Toma-Danila, D.; Riga, E.; Karatzetou, A.; Zucic, Z.; Sousa, L.; Ozcebe, S.; et al. Exposure model for European seismic risk assessment. *Earthq. Spectra* **2020**, *36*, 252–273. [[CrossRef](#)]
2. Calvi, G.M. Choices and Criteria for Seismic Strengthening. *J. Earthq. Eng.* **2013**, *17*, 769–802. [[CrossRef](#)]
3. Wenk, T. *Seismic Retrofitting of Structures, Strategies and Collection of Examples in Switzerland*; Environmental Studies No. 0832; Federal Office for the Environment: Bern, Switzerland, 2008.
4. Tomić, I.; Vanin, F.; Beyer, K. Uncertainties in the Seismic Assessment of Historical Masonry Buildings. *Appl. Sci.* **2021**, *11*, 2280. [[CrossRef](#)]
5. Zhang, S.; Taheri Mousavi, S.M.; Richart, N.; Molinari, J.-F.; Beyer, K. Micro-mechanical finite element modeling of diagonal compression test for historical stone masonry structure. *Int. J. Solids Struct.* **2017**, *112*, 122–132. [[CrossRef](#)]
6. Godio, M.; Stefanou, I.; Sab, K.; Sulem, J.; Sakji, S. A limit analysis approach based on Cosserat continuum for the evaluation of the in-plane strength of discrete media: Application to masonry. *Eur. J. Mech. A/Solids* **2017**, *66*, 168–192. [[CrossRef](#)]
7. Martakis, P.; Reuland, Y.; Imesch, M.; Chatzi, E. Reducing uncertainty in seismic assessment of multiple masonry buildings based on monitored demolitions. *Bull. Earthq. Eng.* **2022**, 1–42. [[CrossRef](#)]
8. Asteris, P.G.; Moropoulou, A.; Skentou, A.D.; Apostolopoulou, M.; Mohebkhah, A.; Cavaleri, L.; Rodrigues, H.; Varum, H. Stochastic Vulnerability Assessment of Masonry Structures: Concepts, Modeling and Restoration Aspects. *Appl. Sci.* **2019**, *9*, 243. [[CrossRef](#)]

9. Vanin, F.; Penna, A.; Beyer, K. A three-dimensional macroelement for modelling the in-plane and out-of-plane response of masonry walls. *Earthq. Eng. Struct. Dyn.* **2020**, *49*, 1365–1387. [[CrossRef](#)]
10. Sarhosis, V.; Giarlelis, C.; Karakostas, C.; Smyrou, E.; Valkaniotis, S.; Ganas, A. Observations from the March 2021 Thessaly Earthquakes: An earthquake engineering perspective for masonry structures. *Bull. Earthq. Eng.* **2022**. [[CrossRef](#)]
11. Asikoglu, A.; Avsar, O.; Lourenço, P.B.; Silva, L. Effectiveness of seismic retrofitting of a historical masonry structure: Kutahya Kursunlu Mosque, Turkey. *Bull. Earthq. Eng.* **2019**, *17*, 3365–3395. [[CrossRef](#)]
12. Tsiavos, A.; Amrein, P.; Bender, N.; Stojadinovic, B. Compliance-Based Estimation of Seismic Collapse Risk of an Existing Reinforced Concrete Frame Building. *Bull. Earthq. Eng.* **2021**, *19*, 6027–6048. [[CrossRef](#)]
13. Tsiavos, A.; Schlatter, D.; Markic, T.; Stojadinovic, B. Shaking table investigation of inelastic deformation demand for a structure isolated using friction-pendulum sliding bearings. *Structures* **2021**, *31*, 1041–1052. [[CrossRef](#)]
14. Tsiavos, A.; Stojadinovic, B. Constant yield displacement procedure for seismic evaluation of existing structures. *Bull. Earthq. Eng.* **2018**, *17*, 2137–2164. [[CrossRef](#)]
15. Bournas, D. *Innovative Materials for Seismic and Energy Retrofitting of the Existing EU Buildings*; JRC Technical Report; European Commission: Brussels, Belgium, 2018.
16. Singh, M.; Stavridis, A. Nonlinear Analysis of Unreinforced Masonry Structures Strengthened with FRP Strips under In-Plane Lateral Loads. In Proceedings of the 11th International Conference on Natural Hazards & Infrastructure, Chania, Greece, 28–30 June 2016.
17. Minafò, G.; Cucchiara, C.; Monaco, A.; La Mendola, L. Effect of FRP strengthening on the flexural behaviour of calcarenite masonry walls. *Bull. Earthq. Eng.* **2017**, *15*, 3777–3795. [[CrossRef](#)]
18. Aprile, A.; Benedetti, A.; Cosentino, N. Seismic reliability of masonry structures strengthened with FRP materials. In Proceedings of the 8th US National Conference on Earthquake Engineering, San Francisco, CA, USA, 18–22 April 2006; p. 167.
19. Passer, A.; Ouellet-Plamondon, C.; Kenneally, P.; John, V.; Habert, G. The impact of future scenarios on building refurbishment strategies towards plus energy buildings. *Energy Build.* **2016**, *124*, 153–163. [[CrossRef](#)]
20. Ostermeyer, Y.; Naegeli, C.; Heeren, N.; Wallbaum, H. Building inventory and refurbishment scenario database development for Switzerland. *J. Ind. Ecol.* **2018**, *22*, 629–642. [[CrossRef](#)]
21. Sigrist, D.; Deb, C.; Frei, M.; Schlüter, A. Cost-optimal retrofit analysis for residential buildings. *J. Phys. Conf. Ser.* **2019**, *1343*, 012030. [[CrossRef](#)]
22. Swiss Federal Office of Energy, Energy Strategy 2050. Available online: <https://www.bfe.admin.ch/bfe/en/home/policy/energy-strategy-2050.html> (accessed on 9 January 2022).
23. Clemett, N.; Gallo, W.; O'Reilly, G.; Gabbianelli, G.; Monteiro, R. Optimal seismic retrofitting of existing buildings considering environmental impact. *Eng. Struct.* **2022**, *250*, 113391. [[CrossRef](#)]
24. European Parliament; Council of the European Union. *Directive (EU) 2018/844 of the European Parliament and of the Council of 30 May 2018 Amending Directive 2010/31/EU on the Energy Performance of Buildings and Directive 2012/27/EU on Energy Efficiency*; Council of the European Union: Brussels, Belgium, 2018.
25. World Meteorological Organization. *State of Global Climate*; Provisional Report; WHO: Geneva, Switzerland, 2021.
26. European Commission. Directive 2010/31/EU of the European Parliament and of the Council of 19 May 2010 on the energy performance of buildings (recast). *Off. J. Eur. Union* **2010**, *53*, 13–35.
27. Furtado, A.; Rodrigues, H.; Arède, A.; Rodrigues, F.; Varum, H. Interactions between Seismic Safety and Energy Efficiency for Masonry Infill Walls: A Shift of the Paradigm. *Energies* **2022**, *15*, 3269. [[CrossRef](#)]
28. Belleri, A.; Marini, A. Does seismic risk affect the environmental impact of existing buildings? *Energy Build.* **2016**, *110*, 149–158. [[CrossRef](#)]
29. Formisano, A.; Vaiano, G. Combined Energy-Seismic Retrofit of Existing Historical Masonry Buildings: The Novel “DUO System” Coating System Applied to a Case Study. *Heritage* **2021**, *4*, 255. [[CrossRef](#)]
30. Negro, P.; Dimova, S.; Bournas, D.; Tsionis, G.; Strezova, D. Integrated Techniques for the Seismic Strengthening and Energy Efficiency of Existing Buildings: A Pilot Project. In Proceedings of the 17th World Conference on Earthquake Engineering (17WCEE), Sendai, Japan, 13–18 September 2020.
31. Caprino, A.; Lorenzoni, F.; Canieletto, L.; Feletto, L.; De Carli, M.; Da Porto, F. Integrated Seismic and Energy Retrofit Interventions on a URM Masonry Building: The Case Study of the Former Courthouse in Fabriano. *Sustainability* **2021**, *13*, 9592. [[CrossRef](#)]
32. Triantafyllou, T.C.; Karlos, K.; Kefalou, K.; Argyropoulou, E. An innovative structural and energy retrofitting system for URM walls using textile reinforced mortars combined with thermal insulation: Mechanical and fire behaviour. *Constr. Build. Mater.* **2017**, *133*, 1–13. [[CrossRef](#)]
33. Caruso, M.; Pinho, R.; Bianchi, F.; Cavalieri, F.; Lemmo, M.T. Integrated economic and environmental building classification and optimal seismic vulnerability/energy efficiency retrofitting. *Bull. Earthq. Eng.* **2021**, *19*, 3627–3670. [[CrossRef](#)]
34. Baek, E.; Pohoryles, D.A.; Kallioras, S.; Bournas, D.A.; Choi, H.; Kim, T. Innovative seismic and energy retrofitting of wall envelopes using prefabricated textile-reinforced concrete panels with an embedded capillary tube system. *Eng. Struct.* **2022**, *265*, 114453. [[CrossRef](#)]
35. Gkournelos, D.; Bournas, D.; Triantafyllou, T. *Combined Seismic and Energy Upgrading of Existing Buildings Using Advanced Materials: Case Studies on Reinforced Concrete Buildings in South Europ*; Publications Office of the European Union: Luxembourg, 2019.



36. Ehrhart, T.; Palma, P.; Steiger, R.; Frangi, A. Numerical and experimental studies on mechanical properties of glued laminated timber beams made from European beech wood. In Proceedings of the 2018 World Conference on Timber Engineering, Seoul, Korea, 20–23 August 2018.
37. De Wolf, C.; Fivet, C. Can timber lower the environmental impact of tall buildings? In *Structures and Architecture: Bridging the Gap and Crossing Borders*; CRC Press: Boca Raton, FL, USA, 2019. [CrossRef]
38. Geier, S.; Herres, U.M.; Sturm, U. *Holzbausanierung Zwischen Ortsbilschutz und Energieeffizienz: Ein Roter Faden für Bauherrschaften*; Lignum, Holzwirtschaft Schweiz: Zürich, Switzerland, 2017.
39. Badini, L.; Ott, S.; Aondio, P.; Winter, S. Seismic strengthening of existing RC buildings with external cross-laminated timber (CLT) walls hosting an integrated energetic and architectural renovation. *Bull. Earthq. Eng.* **2022**. [CrossRef]
40. Simões, A.G. Seismic Behaviour of a Pombalino Quarter of Buildings. Ph.D. Dissertation, Instituto Superior Técnico, Universidade de Lisboa, Lisbon, Portugal, 2010.
41. Simões, A.; Bento, R. *Characterization and Classification of Lisbon Old Masonry Buildings*; Report DTC n° 01/2012, ICIST; Technical University of Lisbon: Lisbon, Portugal, 2010.
42. Cardoso, R.; Lopez, M.; Bento, R. Earthquake resistant structures of portuguese old ‘pombalino’ buildings. In Proceedings of the 13th World Conference on Earthquake Engineering, Vancouver, BC, Canada, 1–6 August 2016; p. 918.
43. Jiménez, B.; Saloustros, S.; Pelà, L. Seismic vulnerability index method for hybrid timber–masonry structures. Numerical calibration and application to the city of Valparaiso, Chile. *J. Build. Eng.* **2021**, *44*, 103185. [CrossRef]
44. Müller, K.; Frangi, A. Micro-notches as a novel connection system for timber-concrete composite slabs. *Eng. Struct.* **2021**, *245*, 112688. [CrossRef]
45. Taylor, B.; Barbosa, A.R.; Sinha, A. In-Plane Shear Cyclic Performance of Spline Cross-Laminated Timber–Concrete Composite Diaphragms. *J. Struct. Eng.* **2021**, *147*, 04021148. [CrossRef]
46. Fischer, E.C.; Shephard, A.B.; Shinha, A.; Barbosa, A.R. Design of timber-concrete composite floors for fire. In Proceedings of the 11th International Conference on Structures in Fire (SiF2020), Brisbane, Australia, 30 November–2 December 2020.
47. Dizhur, D.Y.; Giaretton, M.; Giongo, I.; Ingham, J. Seismic retrofit of masonry walls using timber strong backs. *SESOC J.* **2017**, *30*, 30–44.
48. Miglietta, M.; Damiani, N.; Guerrini, G.; Graziotti, G.F. Full-scale shake-table tests on two unreinforced masonry cavity-wall buildings: Effect of an innovative timber retrofit. *Bull. Earthq. Eng.* **2021**, *19*, 2561–2596. [CrossRef]
49. Lagomarsino, S.; Penna, A.; Galasco, A.; Cattari, S. TreMuri program: An equivalent frame model for the nonlinear seismic analysis of masonry buildings. *Eng. Struct.* **2013**, *56*, 1787–1799. [CrossRef]
50. Penna, A.; Lagomarsino, S.; Galasco, A. A nonlinear macroelement model for the seismic analysis of masonry buildings. *Earthq. Eng. Struct. Dyn.* **2014**, *43*, 159–179. [CrossRef]
51. Bracchi, S.; Penna, A. A novel macroelement model for the nonlinear analysis of masonry buildings. Part 1: Axial and flexural behavior. *Earthq. Eng. Struct. Dyn.* **2021**, *50*, 2233–2252. [CrossRef]
52. Bracchi, S.; Galasco, A.; Penna, A. A novel macroelement model for the nonlinear analysis of masonry buildings. Part 2: Shear behavior. *Earthq. Eng. Struct. Dyn.* **2021**, *50*, 2212–2232. [CrossRef]
53. Vamvatsikos, D.; Cornell, C.A. Incremental dynamic analysis. *Earthq. Eng. Struct. Dyn.* **2002**, *31*, 491–514. [CrossRef]
54. Luzi, L.; Lanzano, G.; Felicetta, C.; D’Amico, M.C.; Russo, E.; Sgobba, S.; Pacor, F. *ORFEUS Working Group 5 (2020). Engineering Strong Motion Database (ESM)*; Version 2.0; Istituto Nazionale di Geofisica e Vulcanologia (INGV): Roma, Italy, 2020.
55. Russo, E.; Felicetta, C.; Amico, M.; Sgobba, S.; Lanzano, G.; Mascandola, C.; Pacor, F.; Luzi, L. *Italian Accelerometric Archive v3.2*; Istituto Nazionale di Geofisica e Vulcanologia, Dipartimento della Protezione Civile Nazionale: Roma, Italy, 2022.
56. PEER NGA Strong Motion Database, Pacific Earthquake Engineering Research Center, University of California, Berkeley. Available online: <https://ngawest2.berkeley.edu/> (accessed on 17 April 2022).
57. Ubakus. Available online: <https://www.ubakus.com/en/r-value-calculator/> (accessed on 10 May 2022).
58. Stolz, P.; Frischknecht, R. Umweltkennwerte und Primärenergiefaktoren von Energiesystemen KBOB. *KBOB-Ökobilanzdatenbestand V.2.2.* 2017, p. 82. Available online: [http://treeze.ch/fileadmin/user\\_upload/downloads/Publications/Case\\_Studies/Energy/563-Energiesysteme-v1.0.pdf](http://treeze.ch/fileadmin/user_upload/downloads/Publications/Case_Studies/Energy/563-Energiesysteme-v1.0.pdf) (accessed on 13 May 2022).
59. *SIA 380/1*; Heizwärmebedarf. Schweizerischer Ingenieur- und Architektenverein: Zürich, Switzerland, 2016.
60. Pittau, F.; Krause, F.; Lumia, G.; Habert, G. Fast-growing bio-based materials as an opportunity for storing carbon in exterior walls. *Build. Environ.* **2018**, *129*, 117–129. [CrossRef]
61. Galimshina, A.; Moustapha, M.; Hollberg, A.; Padey, P.; Lasvaux, S.; Sudret, B.; Habert, G. Bio-based materials as a robust solution for building renovation: A case study. *Appl. Energy* **2022**, *316*, 119102. [CrossRef]
62. Nunes, L. Nonwood bio-based materials. In *Performance of Bio-based Building Materials*; Woodhead Publishing: Sawston, UK, 2017; pp. 97–186.
63. Products/Technical Specifications. Clean Insulating Technologies SA, Lausanne. Available online: <https://gramitherm.ch/?lang=en> (accessed on 7 June 2022).
64. Silvestre, J.D.; Pargana, N.; de Brito, J.; Pinheiro, M.D.; Durão, V. Insulation Cork Boards–Environmental Life Cycle Assessment of an Organic Construction Material. *Materials* **2016**, *9*, 394. [CrossRef]
65. Soares, B.; Reis, L.; Sousa, L. Cork composites and their role in sustainable development. *Procedia Eng.* **2011**, *10*, 3214–3219. [CrossRef]



66. Guerrini, G.; Senaldi, I.; Graziotti, F.; Magenes, G.; Beyer, K.; Penna, A. Shake-Table Test of a Strengthened Stone Masonry Building Aggregate with Flexible Diaphragms. *Int. J. Archit. Herit.* **2019**, *13*, 1078–1097. [[CrossRef](#)]
67. Carofilis, W.; Gabbianelli, G.; Monteiro, R. Assessment of multi-criteria evaluation procedures for identification of optimal retrofitting strategies for existing RC buildings. *J. Earthq. Eng.* **2021**, 1–34. [[CrossRef](#)]
68. Caterino, N.; Iervolino, I.; Manfredi, G.; Cosenza, E. Multi-Criteria Decision Making for Seismic Retrofitting of RC Structures. *J. Earthq. Eng.* **2008**, *12*, 555–583. [[CrossRef](#)]
69. Santarsiero, G.; Masi, A.; Manfredi, V.; Ventura, G. Requalification of RC Frame Apartment Buildings: Comparison of Seismic Retrofit Solutions Based on a Multi-Criteria Approach. *Sustainability* **2021**, *13*, 9962. [[CrossRef](#)]
70. Gentile, R.; Galasso, C. Shedding some light on multi-criteria decision making for seismic retrofitting of RC buildings. In Proceedings of the 2019 Society for Earthquake and Civil Engineering Dynamics Conference (SECED 2019), London, UK, 9–10 September 2019; p. 10.
71. Carofilis Gallo, W.W.; Clemett, N.; Gabbianelli, G.; O'Reilly, G.; Monteiro, R. Seismic Resilience Assessment in Optimally Integrated Retrofitting of Existing School Buildings in Italy. *Buildings* **2022**, *12*, 845. [[CrossRef](#)]
72. Almeida, J.P.; Beyer, K.; Brunner, R.; Wenk, T. Characterization of mortar–timber and timber–timber cyclic friction in timber floor connections of masonry buildings. *Mater. Struct.* **2020**, *53*, 51. [[CrossRef](#)]